Journal of Alloys and Compounds 603 (2014) 42–47

Contents lists available at ScienceDirect

Journal of Alloys and Compounds

journal homepage: www.elsevier.com/locate/jalcom

Strengthening mechanism of two-phase titanium alloys with basketweave microstructure

S.X. Liang [a,b,*], L.X. Yin [b], R.J. Jiang [b], X.Y. Zhang [a], M.Z. Ma [a], R.P. Liu [a,*]

[a] Key Laboratory of Metastable Materials Science and Technology, Yanshan University, Qinhuangdao 066004, China
[b] College of Equipment Manufacture, Hebei University of Engineering, Handan 056038, China

ARTICLE INFO

Article history:
Received 6 February 2014
Received in revised form 8 March 2014
Accepted 12 March 2014
Available online 20 March 2014

Keywords:
Two-phase materials
Strength mechanism
Microstructure
Titanium alloy

ABSTRACT

The Ti–Zr–Al–V (TZAV) series alloys having good mechanical properties are potential structural material to apply in the aerospace industry. The strengthening mechanism of those two-ductile phase TZAV alloys with basketweave (BW) microstructure is crucial to their applications in aerospace industry. As a representative of the TZAV series alloys, Ti–30Zr–5Al–3V (TZAV-30) alloy is used for the strengthening mechanism research of TZAV series alloys with BW microstructure. Various heat treatments were designed to obtain different microstructure and tensile properties. XRD patterns show that all heat treated TZAV-30 specimens are wholly composed by two ductile phases, namely, α phase and β phase, no other phase, such as intermetallic compound, is detected. SEM images show that microstructures of all heat treated TZAV-30 specimens are typical BW microstructures. Results show that strength of the TZAV-30 alloy with BW microstructure is greatly dependent on the thickness of the plate α phase and volume fraction of the retained β phase, but nearly independent on the original β phase grain size. A new strategy to determine the microstructure-strength relationship by focusing on the strength of typical two-ductile-phase alloys with BW microstructures is developed. This relationship can be used to analyze the major influencing factors of strength and to forecast the trend of strength in alloys with various BW microstructures.

1. Introduction

Titanium (Ti) and Ti alloys having low density, high strength, anticorrosion, low temperature resistant and so on excellent physicochemical properties are used extensively in aviation, chemical engineering, medical and other industries. Elements Zirconium (Zr) and Ti belonging to the same group in the element periodic table have the similar physicochemical properties. Lots of investigations have been performed on the effects of Zr on the microstructure and properties of Ti and Ti alloys. Investigating microstructure and properties of the Ti–Zr binary alloys (Zr from 0 to 40 wt%), Ho et al. [1] noted that the hardness, strength and wear resistance of that binary alloy increase with the Zr content. Hsu et al. [2] also showed that phase composition and mechanical properties of the as-casted Zr–Ti binary alloys (Ti from 0 to 40 wt%) vary with the Ti content, and the hardness and bending strength of as-casted Zr–Ti alloys present an obvious decrease as the Ti content increases to 20 wt% resulting in the retained β phase. Other investigations on structure and properties of multi-component Ti alloys also showed that effects of Zr on microstructure and properties of Ti alloys are significant [3–6] Recently, new ultra-high strength Ti–Zr–Al–V (TZAV) series alloys [7–10] were developed, among which the strength of the Ti–20Zr–6.5Al–4V (wt%, TZAV-20) and Ti–30Zr–5Al–3V (wt%, TZAV-30) alloys is over 1600 MPa. Those ultra-high strength TZAV series alloys show a good potential in industrial application.

Research on the strength mechanism of new alloys is very important for the control of mechanical properties and industry applications. Microscopic dislocation theories together with experimental measurements assist in developing specific models [11,12] and laws [13–15] in order to explain the strength of materials, among which the semi-empirical Hall–Petch relationship [16,17] is widely accepted to associate grain size with strength. Lots of other results also demonstrated the significant effects of microstructure on mechanical properties, especially strength. Investigating the microstructure and mechanical properties of the cold rolled and aged Ti–30Nb–5Ta–6Zr alloy, Wang et al. [18] showed that the strength of cold rolled and aged samples increased with decreasing average size of lenticular precipitation α phase. Nie [19] developed the Orowan equation appropriate for magnesium alloys through

* Corresponding authors. Address: College of Equipment Manufacture, Hebei University of Engineering, Handan 056038, China. Tel.: +86 310 8577971; fax: +86 310 8577966.

E-mail addresses: liangshx@hebeu.edu.cn (S.X. Liang), riping@ysu.edu.cn (R.P. Liu).

http://dx.doi.org/10.1016/j.jallcom.2014.03.057
0925-8388/

both theoretical and experimental studies, and results showed that the shape and orientation of precipitates remarkably influence the alloy strength. Besides the hard and brittle second phase mentioned above, the ductile second phase is also crucial for two-phase alloy strength. Gong [20] investigated some factors governing the strength of Ti-based alloys, and results emphasize the importance of the second-phase in alpha-Ti.

The new TZAV series alloys are consist of two ductile solid solution phases, namely, α phase and β phase and are majorly characterized as the typical BW microstructure. Few studies on strengthening mechanism of the TZAV series alloys with BW microstructure have been reported. In the current paper, various heat treatments are designed to perform on the TZAV-30 alloys, a representative of the TZAV series alloys, to study the strength mechanism of TZAV alloys with BW microstructure.

2. Experimental procedure

Sponge Zr (Zr + Hf ⩾ 99.5 wt%), sponge Ti (99.7 wt%), industrial pure Al (99.5 wt%), and vanadium (V) (99.9 wt%) were used to prepare TZAV-30 alloy. The alloy was melted thrice with a ZHT-001 vacuum consumable electro-arc furnace to ensure uniform chemical composition. Multiple breakdowns were performed after holding at 1323 K above the β-transit temperature for 1.5 h to fully break the coarse grain. Final heat forging was performed after holding at 1200 K for 1.5 h, and the ingot was forged into 43 mm-diameter bars. The bars were sectioned into 10 mm × 10 mm × 70 mm segments as heat-treated specimens. Heat treatments were performed in a SK-G06143 tubular vacuum heat treatment furnace with a protective argon atmosphere. Specimens were heated from room temperature to designed holding temperature $T_{holding}$ at the rate 10 K/min, and held at $T_{holding}$ for various times $t_{holding}$, then cooled to 500 °C followed by air cooling. Here the $t_{holding}$ is the duration at $T_{holding}$, cooling rate is the average rate cooling from $T_{holding}$ to 500 °C. Plate specimens with a 21 mm gauge length, 3 mm gauge width, and 2 mm gauge thickness were prepared for tensile tests.

Phase structures were examined by X-ray diffraction (XRD) using Cu Kα radiation. Scanning electron microscopy (SEM) was used for microstructural analysis. The grain size of the α phase was the average values of those incised by two diagonals of each SEM microstructural image. The volume fraction of the retained β phase was tested by the point-counting method. The SEM image of the microstructure was covered by a suitable grid. The ratio of the number of grid points located at the β phase to the total number of grid points was regarded as the volume fraction of the retained β phase. Tensile tests were conducted on an Instron mechanical testing system at room temperature, and the strain rate was $5 \times 10^{-4}\ s^{-1}$. The strain throughout the entire testing process was monitored with an extensometer 12.5 mm in gauge length.

To avoid the contingency, all tests on each specimen were tested at least three times repeatedly and data points in figures are the average values. The error bars in figures show the relative deviations between those three repetitive results and the average value.

3. Results

3.1. Microstructures

Fig. 1 shows XRD patterns of the TZAV-30 specimens annealed at 1123 K and cooled in air, as well as at 10 K/min and 0.35 K/min. All annealed TZAV-30 specimens exhibit the main peaks of α phase with hexagonal close-packed (hcp) structure, as reported for Zr and/or Ti alloys [21–23]. The shift of peak position in TZAV-30 specimens compared with the diffraction peak of Zr and/or Ti alloys confirms the formation of solid solutions. Large solute atoms shift the peaks to the left, and vice versa. Apart from the peaks of the α phase, the obvious peaks at 2θ near 38° and 55° indicate the existence of the β phase with a body-centered cubic (bcc) structure. The relative content of a phase in mixtures can be evaluated by the relative intensity of a diffraction peak of the phase. When we take the peak at 2θ = 55° for the three cases, the relative content of the retained β phase in annealed alloy shows marked differences with various cooling rates. No other peak is detected, indicating that the annealed TZAV-30 alloy is entirely composed of α (hcp structure) and β (bcc structure) phases.

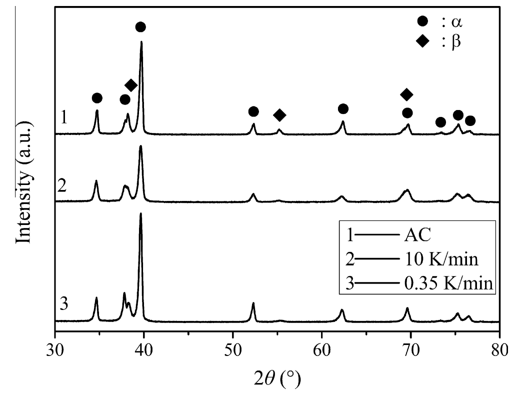

Fig. 1. XRD patterns of 1123 K annealed TZAV-30 specimens after cooling at various rates. AC is the short form of air cooling.

Fig. 2 shows SEM microstructural images of TZAV-30 specimens annealed at 1123 K and cooled in air, as well as at 10 K/min and 0.35 K/min. Remarkably, typical BW microstructures are obvious in the annealed TZAV-30 specimens [24], and the thickness of the α phase noticeably changes with decreased cooling rate. The SEM images reveal the topographic parameters (thickness of the α phase and volume fraction of the retained β phase) obtained using the traditional metallographic measuring methods [25], linear-intercept method, and point-counting method. The results are shown in Table 1. The thickness of the α phase h increases from 0.85 to 10 μm, to the contrary, the volume fraction of the retained β phase f_β decreases from 43.2% to 23.5% with the decrease of cooling rate. Table 2 is the results of the grain size of the original β phase $d_{\beta\text{-orig}}$ from the SEM microstructural images (did not show here) of TZAV-30 specimens holding at 1123 K for 10, 30, 60, and 120 min. The $d_{\beta\text{-orig}}$ in TZAV-30 specimen increases from 100 to 203 μm as the holding time $t_{holding}$ increases form 10 to 120 min.

3.2. Mechanical properties

Fig. 3 shows the tensile stress–strain curves of TZAV-30 specimens with various heat treatments. According to the stress–strain curves, the yield strength of TZAV-30 specimens remains unchanged with the holding time in Fig. 3(a). However, the strength of specimens remarkably decreases from 1137 to 988 MPa with decreased cooling rate in Fig. 3(b).

4. Discussion

The yield strength $\sigma_{0.2}$ of TZAV-30 specimens holding at 1123 K for various time derived from the stress–strain curves in Fig. 3(a) and the grain sizes of the original β phase $d_{\beta\text{-orig}}$ in corresponding specimens are listed in Table 3. The variation in yield strength $\sigma_{0.2}$ is surprisingly very limited, indicating the weak dependence of the TZAV-30 alloy strength on grain size of the original β phase $d_{\beta\text{-orig}}$. This result is unexpected using the Hall–Petch formula $\sigma = \sigma_0 + Kd^{-1/2}$, where the alloy strength is proportional to $-1/2$ powers of grain size. Apparently, the Hall–Petch formula fails to explain the two-ductile-phase alloy with BW microstructure. Generally, fine grains induce additional grain boundaries, which hinder dislocation slips and lead to enhanced alloy strength. The deformation resistance increases with decreased grain size by shortening the distance between the dislocation source and grain boundary, as well as by reducing the dislocation density resulting from dislocation pile-ups on grain boundaries. However, in the examined TZAV-30 specimens, a mass of α phase precipitates inside the original β phase and produces numerous α/β phase